PACS numbers: 42.55.Lt; 42.60.Lh
DOI: 10.1070/QE2008v038n09ABEH013812

Influence of small oxygen additions on the small-signal-gain dynamics in the active medium of a pulsed electron-beam-controlled discharge CO laser

A.A. Ionin, Yu.M. Klimachev, A.Yu. Kozlov, A.A. Kotkov,
A.K. Kurnosov, A.P. Napartovich, S.L. Shnyrev

***Abstract*. The method for measuring the rate constants of the VV′ exchange between CO and O_2 molecules is developed. The method is based on a comparison of the measured and numerically calculated small-signal-gain (SSG) dynamics in the active medium of a pulsed electron-beam-controlled cryogenic CO laser. The SSG dynamics was measured in CO – He – O_2 mixtures with the fixed CO : He = 1 : 4 ratio by varying the oxygen content from 0 to 4 %. The SSG dynamics was measured by probing the active medium of the pulsed CO laser by a beam from a tunable cw CO laser. The mathematical model of the CO laser takes into account the influence of oxygen on energy exchange processes. The parameters of the analytic approximation for constants of the near-resonance VV′ exchange $CO(v) + O_2(u = 0) \rightarrow CO(v - 1) + O_2(u = 1)$ are determined by the developed method for quantum vibrational numbers $v = 18 - 24$. In particular, the rate constant for $v = 20$ is $(3.1 \pm 0.5) \times 10^{-12}$ cm^3 s^{-1} at the gas temperature of 150 K. The extrapolation of the obtained analytic expression for rate constants in gases at room temperature gives the reasonable agreement with the measurements performed earlier for $v = 12$ and 13.**

Keywords: *rate constants, VV′ exchange, oxygen, gain dynamics, electron-beam-controlled CO laser.*

1. Introduction

The influence of oxygen on the parameters of a self-sustained-discharge-pumped CO laser has been often discussed in the literature. In particular, it was found that small additions of O_2 lead to the increase in the output power of the laser [1 – 5]. However, the physical mechanism of this effect is not conclusively established. The main hypotheses proposed to explain it assume that oxygen favours the chemical purification of the laser medium from the products of plasma-chemical reactions, which increase the relaxation rate of vibrationally excited CO molecules [6] and also that a change in the ion composition of the discharge plasma {for example, the replacement of the main ion $(CO)_n^+$ ($n = 2, 3, 4$) by O_2^+ [5, 7]} reduces the electron energy in the discharge and leads to more efficient vibrational excitation of CO molecules. The addition of O_2 molecules to the active medium of the CO laser causes a change in the vibrational distribution function (VDF) of CO molecules because the population of the vibrational levels of CO considerable depends on the rate of kinetic processes of the intermolecular vibrational – vibrational VV′ exchange, VT relaxation, in particular, in collisions of CO molecules with oxygen atoms.

In [8], where the stationary VDF of CO molecules was measured in a self-sustained glow discharge in the CO – He and CO – He – O_2 mixtures, it was shown that the addition of oxygen to the mixture resulted in a drastic decrease in the population of vibrational levels of CO molecules with $v \geqslant 20$ during a gradual transition from the CO : He : O_2 = 1.5 : 12.5 : 0.25 mixture to the CO : He : O_2 = 1.5 : 12.5 : 1 mixture. The authors [8] explained this effect exclusively by the VT relaxation of vibrationally excited molecules by oxygen atoms produced in the self-sustained discharge. Note that due to the anharmonicity of vibrations, the energy of the $22 \rightarrow 21$ vibrational transition in the $^{12}C^{16}O$ molecule becomes almost equal to the energy of the $0 \rightarrow 1$ vibrational transition in the $^{16}O_2$ molecule, which suggests that the efficient quasi-resonance energy transfer can occur during the VV′ exchange processes:

$$CO(v) + O_2(u = 0) \rightarrow CO(v - 1) + O_2(u = 1). \qquad (1)$$

In paper [9] devoted to the diagnostics of a low-temperature plasma in CO-containing mixtures, it was pointed out that a decrease in the vibrational population of CO(v) molecules for $v > 18$ observed after the addition of small amounts of molecular oxygen to the working mixture can be explained by the VV′ exchange between CO and O_2.

The general mechanism of efficient relaxation of the vibrational energy in the active medium of a CO laser containing diatomic impurity molecules with smaller vibrational quanta was discussed earlier in [10]. It was shown, in particular, that at low concentrations ($\sim$1 %) of a diatomic molecular impurity, the VV′ exchange can noticeably reduce the vibrational population of CO molecules at the levels where the VV′ exchange is characterised by the minimal energy defect and also at higher vibrational levels.

However, the inclusion of processes (1) to a numerical model is complicated because data on the rate constants of these processes available in the literature are scarce. The

A.A. Ionin, Yu.M. Klimachev, A.Yu. Kozlov, A.A. Kotkov P.N. Lebedev Physics Institute, Russian Academy of Sciences, Leninsky prosp. 53, 119991 Moscow, Russia; e-mail: aion@sci.lebedev.ru;
A.K. Kurnosov, A.P. Napartovich, S.L. Shnyrev State Research Center of the Russian Federation 'Troitsk Institute for Innovation and Fusion Research', 142190 Troitsk, Moscow region, Russia;
e-mail: apn@triniti.ru

Received 6 February 2008
Kvantovaya Elektronika **38** (9) 833 – 839 (2008)
Translated by M.N. Sapozhnikov

scatter in the values of rate constants of processes (1) for $1 \leqslant v \leqslant 8$ achieves a few orders of magnitude [11]. For $v = 12$ and 13, the rate constants were measured in paper [12], while for $v > 13$ the data are absent in the literature. This situation is explained both by the complexity of populating considerably the high vibrational levels of CO molecules under laboratory conditions and by difficulties encountered in the identification of the contributions of VV′ exchange processes for individual vibrational numbers v.

The active medium of an electron-beam-controlled CO laser is a unique object in which large populations of vibrational levels in the region of the VDF 'plateau' up to $v \approx 40$ can be achieved under laboratory conditions at a comparatively high degree of the spatial homogeneity of excitation. The method of measuring the small-signal-gain (SSG) dynamics at individual vibrational–rotational transitions in the active medium of an electron-beam-controlled CO laser [13] is very sensitive to the population difference at neighbouring vibrational levels [14, 15]. The mathematical model of the active medium of this laser [16] provides good agreement with the experimental SSG dynamics observed in a broad range of vibrational transitions in oxygen-free mixtures.

The SSG dynamics in gas mixtures with different oxygen contents used in pulsed electron-beam-controlled CO lasers can be investigated by probing these mixtures by radiation from a tunable cw CO laser. For example, the addition of O_2 to the active medium of an electron-beam-controlled laser resulted in a noticeable decrease in the duration of the time interval in which probe radiation was amplified or absorbed. At the same time, after the addition of a great amount of oxygen (up to 40 %) to the initial gas mixture CO : He = 1 : 4, the maximum SSG increased at some transitions in the bands from $7 \rightarrow 6$ up to $14 \rightarrow 13$ [17]. The change in the SSG dynamics is mainly caused by VV′ exchange processes (1); however, the influence of oxygen is not limited by this. To take into account completely all the factors, it is necessary to modify the mathematical model of the active medium of an electron-beam-controlled CO laser. By analysing experimental data obtained at low concentrations of O_2 at several vibrational–rotational transitions, we can find, by solving the inverse problem, the rate constants of VV′ exchange processes (1) in the region of vibrational numbers v where the influence of these processes on the SSG dynamics is significant. In this paper devoted to the study of the influence of molecular oxygen on the properties of the active medium of a CO laser, we solved the following problems:

(i) The experimental study of the influence of small oxygen additions to the working mixture of an electron-beam-controlled CO laser on the SSG dynamics in the active medium;

(ii) the modification of the mathematical model of the active medium of a pulsed electron-beam-controlled CO laser with the aim to take into account correctly the influence of oxygen;

(iii) the determination of the rate constants of processes (1) in the region of quantum numbers v where the influence of these processes on the SSG dynamics is considerable.

2. Experiment

Experiments were performed by using a pulsed electron-beam-controlled laser with the active medium of length 1.2 m, which was described in detail in [15]. The SSG dynamics was measured in the CO–He–O_2 mixture for the fixed ratio of components CO : He = 1 : 4 and the content of oxygen molecules in the working mixture equal to 0, 0.4 %, 1 %, 2 %, and 4 %. The relative density N_g of gas in a discharge chamber was 0.1 amagat (the gas density under normal conditions is 1 amagat). The working gas mixture was cooled with liquid nitrogen through the side walls of the discharge chamber. The initial gas temperature T_0 in the active-medium region under study before the current pulse was ~110 K. The gas temperature at the centre of the discharge region in the initial mixture increased up to 150 K within 0.1 ms after the onset of a 0.04-ms electron-beam-controlled discharge pulse for the average specific energy supply $\bar{Q} = 240$ J L^{-1} amagat^{-1} and up to 130 K for $\bar{Q} = 130$ J L^{-1} amagat^{-1} [14].

The SSG dynamics in the active medium of a pulsed laser amplifier was measured by the method of laser probing described in detail in [15]. The probe laser beam of diameter ~1 cm was directed along the axis of the discharge chamber of the laser amplifier in the middle of the interelectrode gap of height 9 cm (the discharge region width was 16.5 cm). The probe laser was a tunable low-pressure cryogenic CO laser, which was pumped by a dc gas discharge [15]. The working gas mixture of the probe laser contained a small amount of oxygen molecules (~0.1 %). The probe CO laser emitted at more than 200 spectral lines in the band of fundamental vibrational transitions from $6 \rightarrow 5$ to $32 \rightarrow 31$. The SSG dynamics was studied at lines with close values of the rotational quantum number J (from 13 to 15) for each of the investigated vibrational transitions. The emission spectrum of the probe CO laser was controlled with an IKS-31 spectrometer equipped with a Ge–Au photodetector. The probe beam intensity (no more than 1 W cm^{-2}) was much smaller than the amplification saturation intensity (~10^2 W cm^{-2} [18]) in the active medium of the pulsed laser amplifier. The output signals of PEM-L-3 (Hg–Cd–Zn–Te) photodetectors, which were proportional to the intensity of probe and amplified radiations, were recorded with a Tektronix TDS2014 oscilloscope. Then, the SSG $G(t)$ was calculated from the recorded signals (the instant $t = 0$ corresponded to the onset of the 40-μs electron-beam-controlled discharge pulse). The SSG dynamics was measured at seven vibrational–rotational transitions in the CO molecule: $7 \rightarrow 6$ P(14), $10 \rightarrow 9$ P(15), $14 \rightarrow 13$ P(14), $18 \rightarrow 17$ P(15), $19 \rightarrow 18$ P(13), $21 \rightarrow 20$ P(14), and $24 \rightarrow 23$ P(15).

3. Theoretical model

The detailed theoretical model of a CO laser with the CO–He and CO–N_2 mixtures [16] correctly describes the VV exchange between CO molecules including multiquantum vibrational exchange processes. This model includes the self-consistent solution of the system of kinetic equations for populations of vibrational levels and equations for the translational gas temperature. The VV and VV′ exchange processes, the VT relaxation, the interaction with plasma electrons, spontaneous and stimulated emission, and the change in the gas density caused by thermal expansion are taken into account. The interaction of molecules with electrons is described by using the Boltzmann equation for the energy distribution function of electrons, which is recalculated when plasma parameters are changed. The

vibrational excitation and de-excitation of CO and N_2 molecules, the excitation of electronic states, ionisation and dissociation of molecules are taken into account.

To describe the influence of O_2 additions, the kinetic model of a CO laser was extended to take into account energy exchange between discharge electrons and O_2 molecules and O atoms by solving the Boltzmann equation. The dissociative and three-body attachment processes were included, and the vibrational kinetics also took into account the VV exchange between O_2 molecules and the VV′ exchange between CO and O_2 molecules.

Rate constants of the vibrational energy exchange between oxygen molecules were determined from semi-classical calculations [19]. It was shown that the rate constants of processes $O_2(v+1) + O_2(u) \rightarrow O_2(v) + O_2(u+1)$ can be quite accurately approximated by standard expressions of the Schwartz–Slavsky–Hertzfeld (SSH) theory [20]:

$$K_{v+1,v}^{u,u+1} = K_{1,0}^{0,1} \frac{v+1}{1-(v+1)\delta} \frac{u+1}{1-(u+1)\delta} \exp(-\delta_{VV}|v-u|),$$

where δ is the relative anharmonicity of the O_2 molecule. The 'VV-exchange radius' δ_{VV} is calculated from the expression $\delta_{VV} = 0.427\hbar\omega\delta l_{st}(\mu/T)^{1/2}$, where $\hbar\omega$ is the vibrational quantum; μ is the reduced mass of colliding molecules; l_{st} is the characteristic size of the short-range part of the intermolecular interaction potential; and T is the translational gas temperature. The SSH theory can be applied if the short-range part of the interaction potential dominates at distances making the main contribution to the energy exchange. This condition is fulfilled only at high gas temperatures.

Figure 1 presents the rate constants calculated in [19] for $T = 100$ and 300 K. These data are well approximated by expression (1) with l_{st} set equal to 0.22 Å for $T = 100$ K and to 0.188 Å for $T = 300$ K. In the case of intermediate temperatures, the value of l_{st} is determined by a linear interpolation. The necessity of varying the parameter l_{st} with temperature suggests that the application of expression (1) is limited at low temperatures. Note that the reliability of the rate constants of the VV exchange between O_2 molecules calculated in [19] is open to question. The dynamics of the vibrational population of $O_2(u)$ molecules was measured recently [21] for $u < 5$ and $T = 300$ K. The VV-exchange rate constants obtained from these data by theoretical simulations proved to be 3–5 times greater than those calculated in [19].

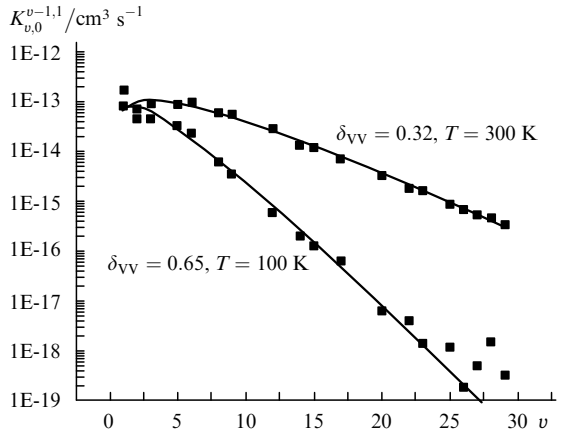

Figure 1. Dependences of the rate constants of the VV exchange in the processes $O_2(v) + O_2 \rightarrow O_2(v-1) + O_2(1)$ on the vibrational quantum number v. The dots are obtained by semi-classical calculations [19].

The data on the rate constants of processes (1) for $v > 13$ are absent in the literature. Based on the qualitative similarity of the interaction potentials for molecular pairs CO–O_2 and CO–N_2, the rates of the VV′ exchange between CO and O_2 were calculated from the analytic expression

$$K_{v,v-1}^{u,u+1} = aZT\frac{v}{1-\delta v}\frac{u+1}{1-[\delta(u+1)]}\exp\frac{\Delta E}{2T} f[y(\Delta E, T)]F + bZ\frac{1}{T}\frac{v}{1-\delta v}|\langle u+1|q|u\rangle|^2 \exp\frac{\Delta E}{2T}\exp\left(-\frac{\Delta E^2}{CT}\right), \quad (2)$$

which was earlier used for calculating the rate constants of near-resonance VV-exchange between CO and N_2 molecules [22, 23]. Here, the first term corresponds to the contribution of the short-range part of the intermolecular interaction potential and the second one – to its long-range part. The parameters entering expression (2) are: $Z = \pi\sigma^2 V_m$ is the gas-kinetic collision constant; V_m is the average velocity of the relative motion of molecules; $\pi\sigma^2$ is the gas-kinetic collision cross section; ΔE is the energy defect of the VV′ exchange process; $\langle u+1|q|u\rangle$ is the matrix element of the quadrupole moment of the O_2 molecule; F is the factor taking into account the attraction of colliding molecules caused by the dispersion (van der Waals) interaction; and $f(y)$ is the adiabatic factor determined by the expression

$$f(y) = 8(\pi/3)^{1/2} y^{7/2}\exp(-3y^{2/3}) \quad \text{for } y \geqslant 21.622$$

or

$$f(y) = 0.5\exp(-2y/3)[3 - \exp(-2y/3)] \quad \text{for } y < 21.622.$$

The Gaussian function of the energy defect $\exp(-\Delta E^2/CT)$ contained in (2) was first proposed in [24] to approximate the VV-exchange rate constants in the case of the dominating long-range part of the interaction potential. The parameters a, c, and C are numerical coefficients, which should be determined for each molecular pair, and $a = 6.61 \times 10^{-8}$ K^{-1}, $b = 4 \times 10^{-2}$ K, and $C = 145$ K for CO–N_2. The factor F and the argument of the adiabatic factor $y(\Delta E, T)$ were calculated as in [25]:

$$y = \left(\frac{16\pi^4\mu l^2|\Delta E|^2}{8h^2kT}\right)^{1/2},$$

$$F = \exp\left(\frac{4}{\pi\sqrt{T^*}}y^{1/3} + \frac{16}{3\pi^2 T^*}\right).$$

Here, l is the characteristic size of the short-range part of the potential equal to 0.203 Å for the CO–N_2 molecular pair [25]; h is Planck's constant; k is the Boltzmann constant; and $T^* = T/\varepsilon$ ($\varepsilon = 100$ K for the CO–N_2 pair).

Analytic expression (2) additively takes into account contributions of the long- and short-range components of the intermolecular interaction potential. The use of this expression for the CO–N_2 pair gave good agreement between experimental VV′-exchange rate constants [26] and semi-classical calculations [22].

Expression (2) for the rate constants of VV′ exchange between vibrationally excited CO molecules and unexcited O_2 molecules can be simplified by excluding from it the first term determining the contribution of the short-range interaction. The temperature of the medium after the end of the pump pulse under our experimental conditions did not exceed 160 K. Therefore, as follows from (2), this contribution is an order of magnitude smaller than the contribution of the long-range dipole–quadrupole interaction for near-resonance exchange processes $CO(v) + O_2 \rightarrow CO(v-1) + O_2(1)$ (for $v > 18$). These two contributions become comparable only for levels with $v < 12$, i.e. for the group of levels where the VV′ exchange is in fact insignificant. As a result, we calculated the VV′-exchange constants from the expression

$$K_{v,v-1}^{u,u+1} = bZ\frac{1}{T}\frac{v}{1-\delta v}(u+1)\exp\frac{\Delta E}{2T}\exp\left(-\frac{\Delta E^2}{CT}\right). \qquad (2a)$$

Here, the expansion of the quadrupole moment in the deviation from the equilibrium is used and the linear term is taken into account [27]. Because this expression is employed for the lowest vibrational levels of O_2, the anharmonicity of oxygen molecules is neglected in it. In this approximation, the dependences of the rate constants on the gas temperature and the level number are characterised by parameters b and C. The first parameter determines the rate constant of the resonance VV′ exchange, while the second one determines the effective half-width of the 'resonance' peak. Unlike the $CO-N_2$ molecular pair, in which the VV′ exchange between N_2 and CO molecules at low excited vibrational levels plays a dominant role, the VV′ exchange in the $CO-O_2$ pair occurs most rapidly for the CO levels with $v \sim 20$ (near the resonance). Note that expression (2a) contains the square of the matrix element of the dipole moment $v/(1-\delta v)$ of the CO molecule, which is much greater at high vibrational levels than at low levels. This suggests that the VV′ exchange of CO with unexcited O_2 molecules will occur much more rapidly than the process $CO(v=1) + N_2(u=0) \rightarrow CO(v=0) + N_2(u=1)$.

We calculated the time dependence of the pump power by using the experimental shapes of the electron-beam-controlled discharge current pulse and of the initial and final voltage pulses on a capacitive storage with the capacitance $C_0 = 55$ μF. The shape of the discharge current pulse $I(t)$ was measured with a low-inductance bifilar shunt. Because the leading edge of this pulse was noisy, we used its analytic approximation in calculations. Figure 2 presents the polynomial approximation of the current pulse $I(t)$, which was measured for $\bar{Q} = 240$ J L^{-1} amagat^{-1} for five oxygen concentrations in the working gas mixture. The pump power and energy supply found in this way are the averaged parameters of the electron-beam-controlled discharge. The authors of paper [16] compared all the experimental data on the SSG dynamics with theoretical calculations and showed that the local specific energy supply Q at the centre of a discharge chamber was smaller approximately by 35 % than the specific energy supply $\bar{Q}$ averaged over the discharge region volume. This is related to the spatial inhomogeneity of the high-energy electron beam current and the pump power in the non-self-sustained discharge.

Because we performed experiments by using the same setup as in [16], corrections for the inhomogeneity of the discharge were calculated by the same method. The average values of the discharge power and energy supply, which were found as described above, were changed by the renormalisation of the dependence $I(t)$. By changing the normalisation, we achieved the best agreement of the calculated SSGs with the gains measured in the absence of O_2 impurities and determined the local specific energy supply. It was found that for the average specific energy supply $\bar{Q} = 130$ J L^{-1} amagat^{-1}, the local value was $Q = 83$ J L^{-1} amagat^{-1}. The calculated SSG dynamics at some transitions is compared with measurements in Fig. 3. For

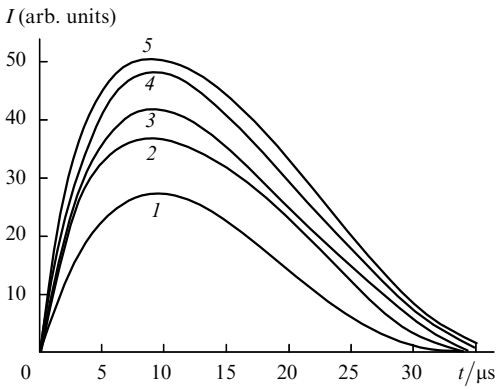

Figure 2. Electron-beam-controlled discharge current pulses ($\bar{Q} = 240$ J L^{-1} amagat^{-1}) approximated by sixth-order polynomials at the concentrations of O_2 in the mixture equal to 0 (*1*), 0.4 % (*2*), 1 % (*3*), 2 % (*4*), and 4 % (*5*).

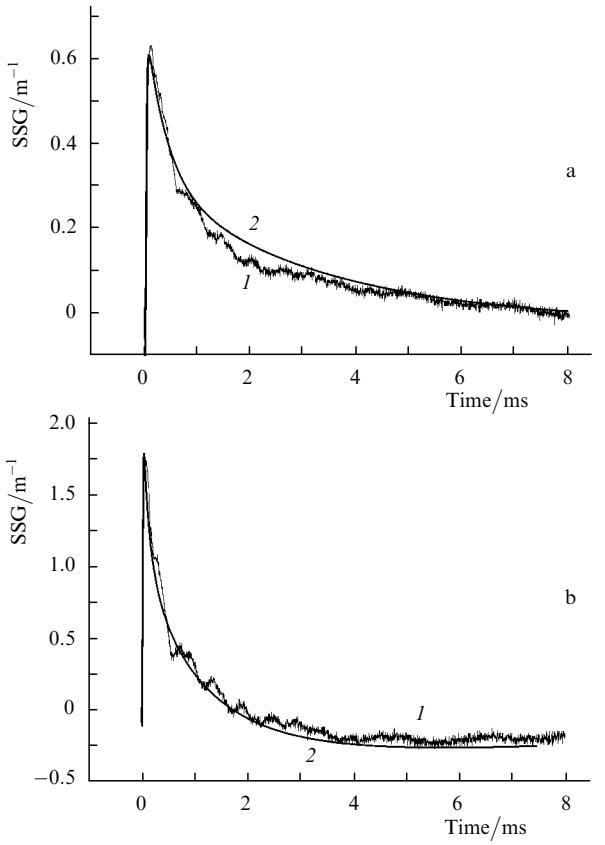

Figure 3. Time dependences of the SSG at the $7 \rightarrow 6$ P(14) (a) and $24 \rightarrow 23$ P(15) transitions (b) for $\bar{Q} = 130$ J L^{-1} amagat^{-1} [(*1*), experiment] and $Q = 83$ J L^{-1} amagat^{-1} [(*2*), calculation].

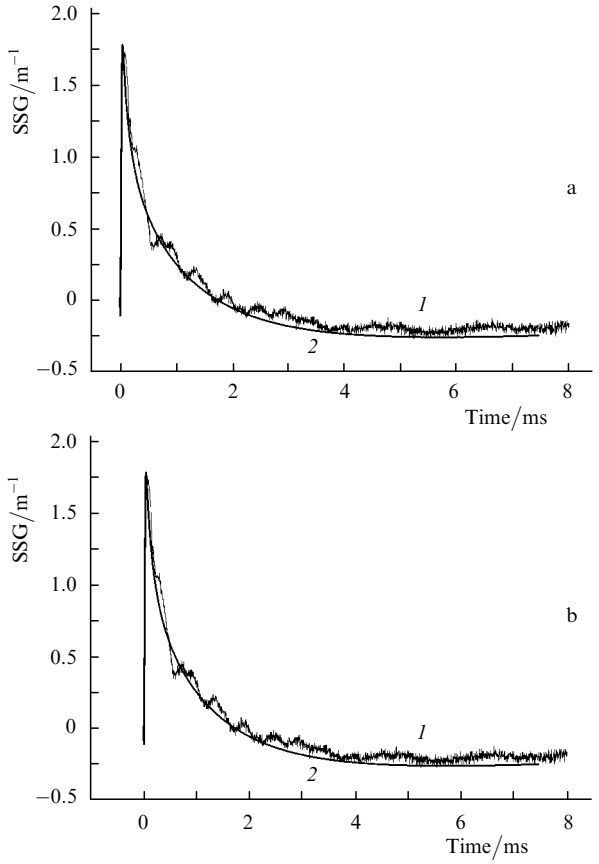

Figure 4. Time dependences of the SSG at the $7 \rightarrow 6$ P(14) (a) and $24 \rightarrow 23$ P(15) transitions (b) for $\bar{Q} = 240$ J L^{-1} amagat^{-1} [(*1*), experiment] and $Q = 142$ J L^{-1} amagat^{-1} [(*2*), calculation].

$\bar{Q} = 240$ J L^{-1} amagat^{-1}, this procedure gives $Q = 142$ J L^{-1} amagat^{-1}. Figure 4 illustrates good agreement between calculations and measurements.

In the presence of oxygen in the working mixture, the VV′-exchange rate for CO and O_2 becomes quite uncertain. It is expected that this exchange makes a considerable contribution to the SSG dynamics. However, estimates by expression (2a) show that the VV′ exchange can make a noticeable contribution to the SSG dynamics only for the CO levels ($v > 18$) for which the difference between the vibrational quanta of O_2 and CO becomes small. Therefore, the results of measuring the SSG dynamics at the $7 \rightarrow 6$, $10 \rightarrow 9$, and $14 \rightarrow 13$ transitions can be used for measuring the local energy supply. The local value of Q in the presence of oxygen was calculated for these transitions by the same method as in the absence of oxygen. One can see from Fig. 5 that the addition of 2 % of oxygen leads to an increase in the gain and only weakly affects the local energy supply. Table 1 presents the values of Q found at different oxygen concentrations. A small difference of the local energy supply from its values in the oxygen-free mixture suggests that the discharge structure weakly changes after the addition of oxygen.

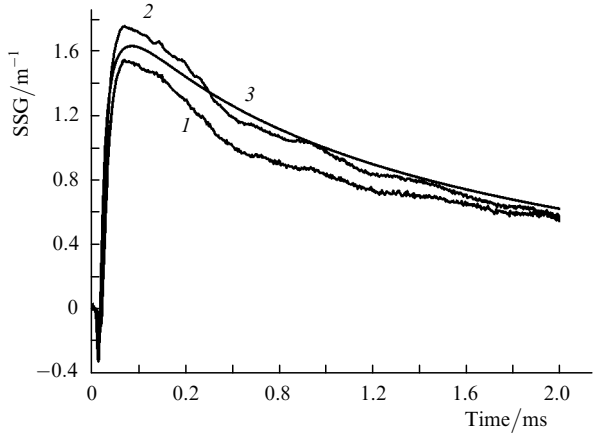

Figure 5. Time dependences of the SSG at the $14 \rightarrow 13$ P(14) transition: (*1*) experiment for $\bar{Q} = 240$ J L^{-1} amagat^{-1} without the addition of oxygen; (*2*) experiment for $\bar{Q} = 240$ J L^{-1} amagat^{-1} and the oxygen concentration 2 %; (*3*) calculation for $Q = 147$ J L^{-1} amagat^{-1} and the oxygen concentration 2 %.

Table 1. Local values of the specific energy supply Q for $\bar{Q} = 130$ J L^{-1} amagat^{-1} (Q_1) and $\bar{Q} = 240$ J L^{-1} amagat^{-1} (Q_2) at different O_2 concentrations in the mixture.

$[O_2]$ (%)	Q_1/J L^{-1} amagat^{-1}	Q_2/J L^{-1} amagat^{-1}
0	83	142
0.4	87	145
1	89	147
2	89	147
4	93	147

4. Determination of the rate constants of quasi-resonance VV′ exchange between CO and O_2 molecules

The time dependences of the SSG measured at seven laser transitions in CO allow us to calculate the rate constants of the VV′ exchange between CO and O_2 near the resonance by using expression (2a) and minimising the difference between the measured and calculated SSGs by selecting coefficients b and C. The initial values of these coefficients were assumed equal to those for the CO–N_2 molecular pair. The calculations of the SSG dynamics for the near-resonance levels ($v \sim 20$) revealed a considerable difference from experimental data. In addition, the calculations showed that the influence of O_2 additions on the SSG dynamics considerably depends on the vibrational level number of CO. At the same time, as expected, the SSG dynamics calculated for the lower $7 \rightarrow 6$, $10 \rightarrow 9$, and $14 \rightarrow 13$ transitions is almost independent of variations in the VV′-exchange rate constants.

Thus, information on the VV′-exchange rate constants can be obtained by analysing the SSG dynamics at transitions with large v. We analysed the data file on the SSG dynamics at each transition with a step of 4 μs at the time interval $t = 48 - 3992$ μs (987 points altogether). The agreement between the results of calculations and experimental data was estimated by using the target function representing the sum of squares of deviations of the calculated SSG values $G_{\text{theor}}(i)$ from experimental values $G_{\text{exp}}(i)$, which was normalised to the sum of squares of the measured SSGs:

$$S^2 = \frac{\sum_{i=1}^{K} \left[G_{\text{theor}}(i) - G_{\text{exp}}(i)\right]^2}{\sum_{i=1}^{K} \left[G_{\text{exp}}(i)\right]^2}, \qquad (3)$$

where $K = 987$.

The value of the target function depends on the parameters b and C by which the function minimum should be found. The values of b were varied with a step of 0.02 K in the interval from 0.08 to 0.30 K. Analysis performed for the $18 \rightarrow 17$ P(15) and $19 \rightarrow 18$ P(13) transitions showed that for the fixed coefficient b the value of C providing the constrained minimum of the target function can be determined quite accurately. The values of parameters b and C found in this way are presented in Table 2. Figures 3–5 show the experimental dependences of the SSG and the corresponding curves calculated for the values of parameters providing the minimum of the target function. It follows from Fig. 6 that for $b = 0.2$ K, a change in the parameter C by less than 20 % noticeably changes the calculated SSG dynamics at the $18 \rightarrow 17$ P(15) transition. This effect is explained by the fact that the transition occurs between the levels located somewhat lower than the resonance level with $v \sim 20$ at which the VV′-exchange rate is maximal. For this region of vibrational levels, the resonance width is obviously an important factor.

By using all the eleven experimental time dependences of the SSG at the $18 \rightarrow 17$ P(15), $19 \rightarrow 18$ P(13), $21 \rightarrow 20$ P(14), and $24 \rightarrow 23$ P(15) transitions at the concentrations of molecular oxygen from 0.4 % to 4 % and for $\bar{Q} = 130$ and 240 J L^{-1} amagat^{-1}, we can find the parameters b and C to a high accuracy. For this purpose, the target function was generalised with the help of the expression

$$F = \frac{1}{N}\sum_{i=1}^{N} S_i^2 ,$$

where $N = 11$ and S_i^2 was found for each transition from (3). Table 2 presents the values of the generalised target function calculated for different combinations of parameters b and C. Taking into account the experimental error, we can conclude that the SSG dynamics at all the transitions is well described by expression (2a) for the values of parameters b and C at which the generalised target function is equal to 0.130–0.149. Figure 7 presents the dependences of the rate constants on v for near-resonance VV′-exchange processes $CO(v) + O_2 \rightarrow CO(v-1) + O_2(1)$ for two sets of parameters b and C. Table 3 presents the recommended VV′-exchange rate constants for $v = 20 - 23$ calculated for $b = 0.20$ K, $C = 120$ K and the translational gas temperature $T = 150$ K.

Table 2. Minimal values of the generalised target function F at different parameters b and C.

b (K)	C (K)	F
0.30	95	0.208
0.28	100	0.182
0.26	105	0.168
0.24	*110*	*0.149*
0.22	115	0.136
0.20	**120**	**0.130**
0.18	130	0.132
0.16	140	0.140
0.14	*145*	*0.147*
0.12	150	0.204
0.10	165	0.267
0.08	180	0.416

Note: values at which the generalised function is minimal are shown in bold; values at which the target function differs from its minimum by 20 % are italicised.

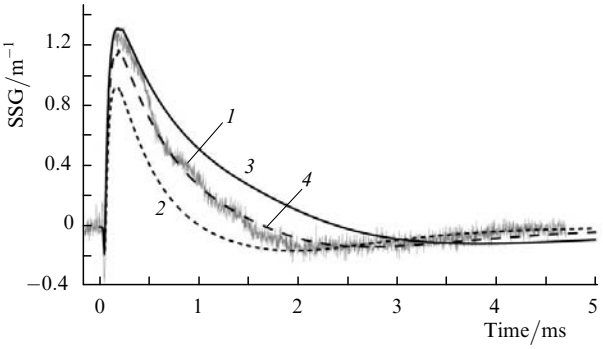

Figure 6. Time dependences of SSG at the $18 \rightarrow 17$ P(15) transition for $\bar{Q} = 240$ J L^{-1} amagat^{-1} and the oxygen concentration 4 %: (*1*) experiment; (*2*) calculation for $b = 0.2$ K and $C = 145$ K; (*3*) calculation for $b = 0.2$ K and $C = 100$ K; (*4*) calculation for $b = 0.2$ K and $C = 120$ K.

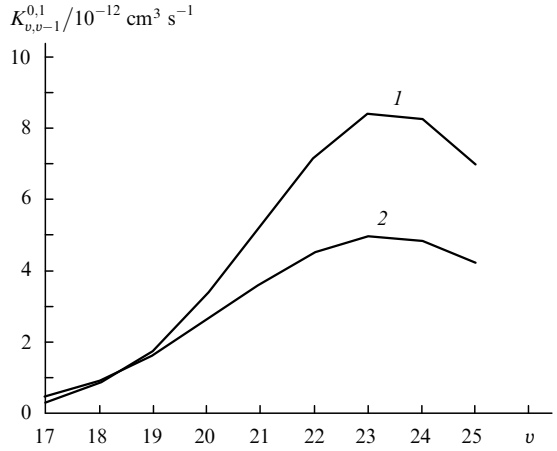

Figure 7. Dependences of the rate constants of the quasi-resonance VV′ exchange on v in the processes $CO(v) + O_2 \rightarrow CO(v-1) + O_2(1)$ for $b = 0.24$ K, $C = 110$ K (*1*) and $b = 0.14$ K, $C = 145$ K (*2*); $T = 150$ K.

Table 3. Recommended rate constants of the VV′ exchange between CO and O_2 molecules at $T = 150$ K.

v	$K^{0,1}_{v,v-1}$/cm^3 s^{-1}
23	$(6.7 \pm 1.8) \times 10^{-12}$
22	$(6.1 \pm 1.6) \times 10^{-12}$
21	$(4.7 \pm 1.0) \times 10^{-12}$
20	$(3.1 \pm 0.5) \times 10^{-12}$

The dependences of the rate constants on the vibrational level number v calculated for $T = 100$, 200, and 300 K are presented in Fig. 8. The rate constants calculated for $T = 300$ K can be compared with data [12] for the VV′ exchange in the processes $CO(v) + O_2 \rightarrow CO(v-1) + O_2(1)$ for $v = 12$ and 13. These data were obtained by processing the measurements of the chemiluminescence intensity in the $O + CS = CO(v = 4 - 13) + S$ reaction. The VV′-exchange rate constants obtained in [12] are 2.1×10^{-14} cm^3 s^{-1} ($v = 12$) and 4.4×10^{-14} cm^3 s^{-1} ($v = 13$). These rate constants obtained in our calculations for $b = 0.2$ K and $C = 120$ K are 2.7×10^{-14} and 6.4×10^{-14} cm^3 s^{-1}, respec-

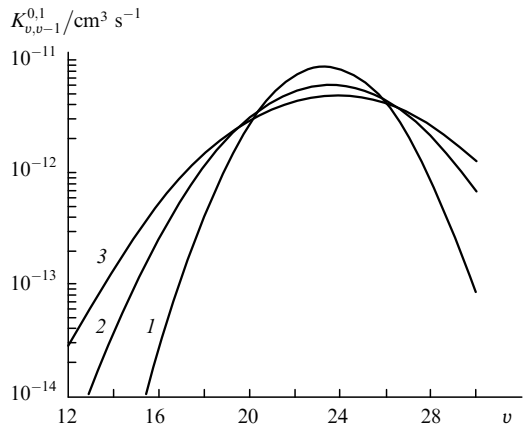

Figure 8. Dependences of the rate constants of the quasi-resonance VV′ exchange in the processes $CO(v) + O_2 \rightarrow CO(v-1) + O_2(1)$ on v calculated by (2a) for $b = 0.20$ K, $C = 120$ K, and $T = 100$ (*1*), 200 (*2*), and 300 K (*3*).

tively. Taking into account that our calculations and calculations performed in [12] were approximate, the agreement between them is quite satisfactory.

5. Conclusions

We have studied the influence of small O_2 additions on the SSG dynamics in the active medium of a pulsed electron-beam-controlled cryogenic CO laser. By using the numerical model of the CO laser, we have determined how the VV′ exchange between CO molecules at high excited vibrational levels and oxygen molecules affects the SSG dynamics. By comparing the measured and calculated SSG dynamics for a number of transitions, we have determined the parameters of the analytic approximation of the VV′-exchange rate constants for the $CO-O_2$ molecular pair at the cryogenic temperature of the active medium. The recalculation of the VV′-exchange rate constants to gas at room temperature by using the analytic approximation gives reasonable agreement with data obtained in [12].

Acknowledgements. This work was partially supported by Grant No. NSh-1573.2008.2 of the President of the Russian Federation for the State Support of the Leading Scientific Schools of the Russian Federation.

References

1. Osgood R.M., Eppers W.C., Nichols E.R. *IEEE. J. Quantum Electron.*, **6**, 145 (1970).
2. Bhaumik M.L., Lacina W.B., Mann M.M. *IEEE J. Quantum Electron.*, **8**, 150 (1972).
3. Keren H., Avivi P., Dothan F. *IEEE. J. Quantum Electron.*, **11**, 590 (1975).
4. Trubachev E.A. *Trudy FIAN*, **102**, 3 (1977).
5. Morgan W.L., Fisher E.R. *Phys. Rev. A*, **16**, 1186 (1977).
6. Grigoryan G.M., Dymshyts B.M., Ionikh Yu.Z. *Kvantovaya Elektron.*, **16**, 1377 (1989) [*Sov. J. Quantum Electron.*, **19**, 889 (1989)].
7. Grigoryan G.M., Ionikh Yu.Z. *Teplofiz. Vys. Temp.*, **35**, 702 (1977).
8. Fisher E.R., Lightman A.J. *J. Appl. Phys.*, **49**, 530 (1978).
9. Plönjes E., Palm P., Adamovich I., Rich W. *J. Phys. D.: Appl. Phys.*, **33**, 2049 (2000).
10. Konev Yu.B., Kochetov I.V., Kurnosov A.K. Preprint of I.V. Kurchatov Institute of Atomic Energy, No. 3995/12 (Moscow, 1984).
11. Wang B., Gu Y., Kong F. *J. Phys. Chem. A*, **102**, 9367 (1998).
12. Hancock G., Smith I.W.M. *Appl. Opt.*, **10**, 1827 (1971).
13. Vetoshkin S.V., Ionin A.A., Klimachev Yu.M., et al. *Kvantovaya Elektron.*, **37**, 111 (2007) [*Quantum Electron.*, **37**, 111 (2007)].
14. Ionin A.A., Klimachev Yu.M., Kozlov A.Yu., et al. *Kvantovaya Elektron.*, **37**, 231 (2007) [*Quantum Electron.*, **37**, 231 (2007)].
15. Vetoshkin S.V., Ionin A.A., Klimachev Yu.M., et al. Preprint FIAN, No. 13 (Moscow, 2005); Vetoshkin S.V., Ionin A.A., Klimachev Yu.M., et al. *J. Rus. Laser Research*, **27**, 33 (2006).
16. Vetoshkin S.V., Ionin A.A., Klimachev Yu.M., et al. *Kvantovaya Elektron.*, **35**, 1107 (2005) [*Quantum Electron.*, **35**, 1107 (2005)].
17. Ionin A.A., Klimachev Yu.M., Kozlov A.Yu., et al. *Kvantovaya Elektron.*, **38**, 115 (2008) [*Quantum Electron.*, **38**, 115 (2008)].
18. Elkin N.N., Kochetov I.V., Kurnosov A.K., Napartovich A.P. *Kvantovaya Elektron.*, **17**, 313 (1990) [*Sov. J. Quantum Electron.*, **20**, 252 (1990)].
19. Coletti C., Billing G.D. *Chem. Phys. Lett.*, **356**, 14 (2002).
20. Capitelli M., Ferreira C.M., Gordiets B.F., Osipov A.I. *Plasma Kinetics in Atmospheric Gases* (Berlin: Springer, 2000).
21. Ahn T., Adamovich I., Lempert W. *Chem. Phys.*, **323**, 532 (2006).
22. Kurnosov A., Cacciatore M., Billing G.D. *J. Phys. Chem. A*, **107**, 2403 (2003).
23. Ionin A.A., Kazakevich V.S., Kovsh I.B., et al. Preprint FIAN, No. 232 (Moscow, 1982).
24. Rockwood S.D., Brau J.E., Proctor W.A., Canavan G.H. *IEEE J. Quantum Electron*, **9**, 120 (1973).
25. Smith N.S., Hassan H.A. *AIAA J.*, **14**, 374 (1976).
26. Allen D.S., Simpson C.I.S.M. *Chem. Phys.*, **45**, 203 (1980).
27. Heaps H.S., Herzberg G. *Zeitschrift fur Physik*, **133**, 48 (1952).